Journal of Organometallic Chemistry 728 (2013) 57–67

Contents lists available at SciVerse ScienceDirect

Journal of Organometallic Chemistry

journal homepage: www.elsevier.com/locate/jorganchem

Rare earth metal complexes anchored on a new dianionic bis(phenolate)dimethylamineCyclam ligand

Leonor Maria [a,b,*], Isabel C. Santos [a], Luís G. Alves [b], Joaquim Marçalo [a], Ana M. Martins [b,*]

[a] Unidade de Ciências Químicas e Radiofarmacêuticas, IST/ITN, Instituto Superior Técnico, Universidade Técnica de Lisboa, 2686-953 Sacavém, Portugal
[b] Centro de Química Estrutural, Instituto Superior Técnico, Universidade Técnica de Lisboa, 1049-001 Lisboa, Portugal

ARTICLE INFO

Article history:
Received 17 October 2012
Received in revised form
7 December 2012
Accepted 12 December 2012

Keywords:
Rare earth metals
Lanthanides
Cyclam derivatives
Bis(phenolate)
Cyclic tetraamines

ABSTRACT

A new bis(phenol)dimethyltetraazamacrocycle, 1,8-bis(2-hydroxy-3,5-di-tert-butylbenzyl)-4,11-dimethyl-1,4,8,11-tetraazacyclotetradecane (H_2{(^{tBu2}PhO)$_2$Me$_2$Cyclam}) (**1**), is described. Deprotonation of **1** with sodium or potassium hydrides afforded Na_2{(^{tBu2}PhO)$_2$Me$_2$Cyclam} (**2**) and K_2{(^{tBu2}PhO)Me$_2$Cyclam} (**3**), respectively. Reactions of **2** or **3** with yttrium or lanthanide trichlorides led to the formation of neutral rare earth metal complexes of general formula [{(^{tBu2}PhO)$_2$Me$_2$Cyclam}LnCl] (Ln = Y (**4**), La (**5**), Sm (**6**), Yb (**7**)) in moderate to high yields. The molecular structures of **4**–**7** were determined by single-crystal X-ray diffraction analysis and reveal that the ligand's denticity depends on the size of the metal ions. The smaller Y^{3+} and Yb^{3+} lead to distorted octahedral geometries where the dianionic ligand acts as pentadentate, while the larger ions, La^{3+} and Sm^{3+}, form capped trigonal prismatic complexes with the cyclam derivative acting as a hexadentate chelator.

1. Introduction

The stability and reactivity of trivalent rare earth metal complexes are largely dominated by the highly electropositive character of the metal ions, as well as the degree of saturation of their coordination sphere. Therefore, the search for bulky ancillary ligands that allow synthesizing new reactive coordination environments is an important topic in rare earth metal chemistry. In this context, the combination of two phenolate groups with fragments bearing N-, O- or S-donors proved to be an adequate strategy for the design of yttrium(III) and lanthanide(III) complexes of general formula LLnR (Ln = Y, La, Nd, Sm, Yb), where R is an alkoxide, aryloxide, amide or alkyl. The thermodynamic and kinetic stability provided by these chelating ligands circumvented ligand redistribution reactions and enable the isolation of well-defined species [1–3] that have been reported and successfully used as catalysts in ring-opening polymerization of cyclic esters [1,2,4] and in intramolecular aminoalkene hydroamination processes [5].

Previous work by some of us showed that the introduction of dianionic cyclam-based ligands in zirconium chemistry [6] widened the catalytic applications of zirconium complexes and revealed new reactivity patterns that are intimately related to the hemilabile behaviour of the tetraazamacrocyclic frame. The flexibility displayed by the macrocycle framework leads to distinct bonding modes and is responsible for the stabilization of different metal coordination geometries, providing new entries to metal mediated reactions [7]. Ln(III) metal complexes derived from tetrasubstituted tetraazamacrocycles, in particular cyclen and cyclam, are widely documented as they display important diagnostic and therapeutic applications [8]. The attachment of anionic O-donor groups to the macrocycle's nitrogens revealed essential for the stabilisation of many complexes that have been used in magnetic resonance imaging (MRI), as luminescent probes in medicine and biology and as radiometal-labelled agents for therapeutic applications [9].

Metal complexes derived from trisubstituted triazacyclonane rings of the type trisamido- or trisphenolate-tacn revealed interesting reactivity profiles [10]. The cavity defined by this type of ligands provides effective steric protection to metal centres, confines incoming reagents and determines its bonding modes [11]. These aspects are well illustrated by ((^{tBu}ArO)$_3$tacn)Ln complexes, for which an unprecedented μ,η^1,η^1-*O,O′* coordination of SO_2 was identified [10a].

In this work we report a new cyclam derivative obtained by *N*-functionalization of the macrocycle with two bulky 2-hydroxy-3,5-di-tert-butylbenzyl pendant arms. Upon deprotonation, this compound is a dianionic hexa-donor of the type $[N_4O_2]^{2-}$ that may potentially coordinate to metals through the four amines of the

* Corresponding authors. Centro de Química Estrutural, Instituto Superior Técnico, Universidade Técnica de Lisboa, 1049-001 Lisboa, Portugal.
E-mail addresses: leonorm@itn.pt (L. Maria), ana.martins@ist.utl.pt (A.M. Martins).

0022-328X/$ – see front matter © 2012 Elsevier B.V. All rights reserved.
http://dx.doi.org/10.1016/j.jorganchem.2012.12.026

cyclam ring and the two anionic O-donors. The ligand precursor, 1,8-bis(2-hydroxy-3,5-di-tert-butylbenzyl)-4,11-dimethyl-1,4,8,11-tetraazacyclotetradecane, was devised aiming at the syntheses of well-defined Y(III) and Ln(III) complexes with general formula [{(^{tBu2}PhO)$_2$Me$_2$Cyclam}MCl] (M = Y, La, Sm, Yb), which are also described.

2. Results and discussion

2.1. Synthesis and characterization of H_2{(^{tBu2}PhO)$_2$Me$_2$Cyclam} and M_2{(^{tBu2}PhO)$_2$Me$_2$Cyclam} (M = Na, K)

As shown in Scheme 1, the ligand precursor 1,8-bis(2-hydroxy-3,5-di-tert-butylbenzyl)-4,11-dimethyl-1,4,8,11-tetraazacyclotetradecane (**1**) (H_2{(^{tBu2}PhO)$_2$Me$_2$Cyclam}) is readily synthesized in four steps starting from cyclam. Two methyl groups were selectively introduced at *trans*-nitrogen atoms of the macrocycle through alkylation of the bisaminal derivative of cyclam with MeI, followed by basic hydrolysis as described by Guilard et al. [12]. The subsequent *N*-alkylation of 1,8-dimethylcyclam with 2-hydroxy-3,5-di-tert-butylbenzyl was achieved with aqueous formaldehyde and 2,4-di-*tert*-butylphenol in refluxing methanol, following a typical Mannich procedure. H_2{(^{tBu2}PhO)$_2$Me$_2$Cyclam} (**1**) precipitates out of solution as a white solid, in 85% yield. **1** is soluble in aromatic solvents, tetrahydrofuran and chlorinated solvents, and sparingly soluble in *n*-hexane and in acetonitrile.

The ^{1}H NMR spectrum of **1** in benzene-d_6, at room temperature, reveals a series of broad resonances that were assigned to ten diastereotopic macrocyclic protons and to two diastereotopic benzyl protons on the basis of ^{1}H–^{13}C HSQC experiments. The observation of one set of resonances for the ^{tBu2}PhOH and the N–CH$_3$ groups confirms that the mutually *trans*-substituents are magnetically equivalent. The carbon NMR spectrum reveals five different methylene carbons assigned to the cyclam frame, one benzyl and one methyl carbon resonances, and one set of signals for the equivalent ^{tBu2}PhOH groups. The high-frequency shift of the OH protons (δ 10.0 ppm) as well as the pattern observed for the macrocycle protons suggests that the ^{tBu2}PhOH groups establish hydrogen bonds with the nitrogen atoms of the cyclam ring. These interactions are responsible for the difference between the two "faces" of the macrocycle and the observation of 10 non-equivalent proton resonances. As a whole the NMR results are compatible either with the presence of a C_2 symmetry molecule or with a C_i symmetry species with an inversion centre in the middle of the cyclam ring. The latter structure, which is observed in the solid state (see below), is likely to be also maintained in solution. Albeit some proton resonances overlap, it was possible to distinguish between the resonances corresponding to the two-carbon [C2] and three-carbon chains [C3] of the macrocycle based on homonuclear and heteronuclear NMR experiments (^{1}H–^{1}H COSY, ^{1}H–^{13}C HSQC, ^{1}H–^{13}C HMBC).

Single crystals of **1** suitable for X-ray diffraction were grown from a dilute acetonitrile solution. The asymmetric unit contains one-half of the molecule with the macrocycle centred on a crystallographic inversion centre (=–x + 1, –y + 1, –z). An ORTEP diagram and most relevant bond lengths and angles are depicted in Fig. 1a.

According to the extended Dale's nomenclature, which takes in account the extended position of the heteroatoms, the 14-membered macrocycle adopts a rectangular conformation (4,3,4,3)-B with C(2), C(5) and symmetry related carbon atoms at the corners of the rectangle (Fig. 1b). The torsion-angles sequence $\tau_1 - \tau_7$ is 40.3(3), 68.8(2), –172.2(2), 175.0(2), –67.1(2), –75.1(2), 169.7(2)°, with τ_1 = N(1)–C(1)–C(2)–N(2) and τ_7 = C(5)–N(1a)–C(1a)–C(2a) [13].

As suggested by the proton NMR spectrum, the structure is stabilized by intramolecular hydrogen bonds involving the phenolic protons and the nitrogen atoms, with N(1)–H(1)O(1) and N(2)–H(1)O(1) distances of 2.251(2) Å and 1.990(2) Å, respectively. H(1) was not found in the Fourier difference map and its position was geometrically fixed but even though the presence of hydrogen bonds may be inferred from the short distances O(1)–N(1) (2.938(2) Å) and O(1)–N(2) (2.886(2) Å). The configurations of the four nitrogen atoms of **1** correspond to a type IV cyclam configuration (S, R, R, S) [14].

Treatment of H_2{(^{tBu2}PhO)$_2$Me$_2$Cyclam} with excess of NaH or KH in THF at room temperature afforded Na_2{(^{tBu2}PhO)$_2$Me$_2$Cyclam}(THF)$_2$ (**2**) and K_2{(^{tBu2}PhO)$_2$Me$_2$Cyclam}(THF)$_2$ (**3**) in quantitative yields. **2** and **3** are soluble in tetrahydrofuran and insoluble in aromatic solvents and *n*-hexane. The room temperature ^{1}H NMR spectrum of **2** in THF-d_8 displays one set of resonances for the two phenolate groups, two resonances for the diastereotopic benzyl protons, one resonance for the NCH$_3$ groups and a complex series of broad resonances that spread from 0.84 ppm to 3.02 ppm for the methylene protons of the cyclam ring. The ^{13}C spectrum is consistent with the proton NMR spectrum and characteristic of average

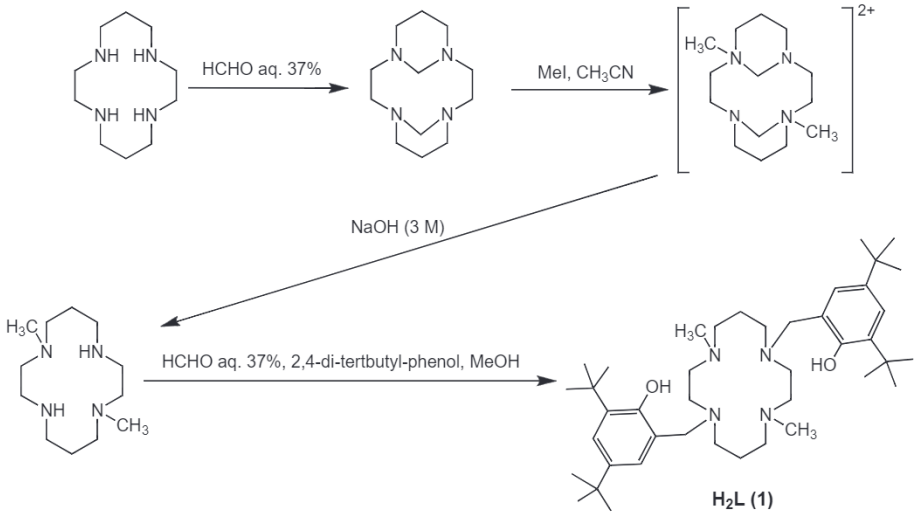

Scheme 1. Synthesis of H_2{(Ar^{tBu2}PhO)$_2$Me$_2$Cyclam} (**1**).

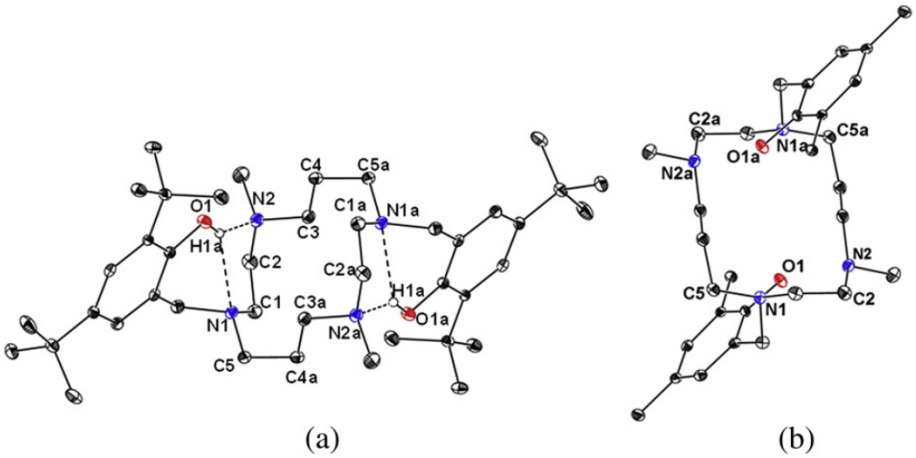

Fig. 1. (a) Molecular structure of H_2[(Ar^{tBu2}PhO)$_2$Me$_2$Cyclam] (**1**). Thermal ellipsoids are drawn at 50% probability level. Selected bond lengths (Å) and angles (°): N(1)–C(7) 1.467(3), N(1)–C(1) 1.463(3), N(1)–C(5) 1.466(3), N(2)–C(6) 1.463(3), N(2)–C(2) 1.464(3), N(2)–C(3) 1.468(3), C(13)–O(1) 1.363(2), C(1)–N(1)–C(5) 111.66(16), C(3)–N(2)–C(2) 111.48(17), C(7)–N(1)–C(1) 111.57(17), C(7)–N(1)–C(5) 110.75(16), C(6)–N(2)–C(3) 111.18(17), C(6)–N(2)–C(2) 109.38(17). (b) Conformation of the cyclam ring in **1** (hydrogens and ^{t}Bu groups are omitted for clarity).

C_2 symmetry in solution, in agreement with the structure determined by single crystal X-ray diffraction (see Fig. 2). The NMR data for **3** are essentially equivalent to those of **2** but the ^{1}H NMR spectrum is poorly resolved. Attempts to attain a static spectrum by lowering the temperature were unfruitful.

Crystals of Na$_2${(Ar^{tBu2}PhO)$_2$Me$_2$Cyclam}(THF)$_2$ (**2**) were obtained from a concentrated THF solution at −20 °C. X-ray diffraction analysis of the crystals revealed that they had poor diffracting power but allowed its unequivocal structural identification. The compound crystallizes with two crystallographically independent molecules in the asymmetric unit (**2a** and **2b**). The two molecules do not differ significantly and for simplicity the discussion refers exclusively to **2a** (crystallographic data for **2b** are presented as Supplementary data, Table S2 and Fig. S2). An ORTEP view is depicted in Fig. 2 and Table 1 summarizes important bonds and angles for **2a**.

The structure shows two differently coordinated sodium centres. Na(1) is bonded to the four nitrogen atoms of the cyclam ring and to two oxygen atoms of the phenolate moieties in a distorted trigonal prismatic geometry. The nitrogen atoms of the cyclam define one rectangular face of the prism with deviations from the average plane shorter than 0.459 Å. The dihedral angle between the two triangular faces O(1)–N(1)–N(4) and O(2)–N(2)–N(3) is 5.9°.

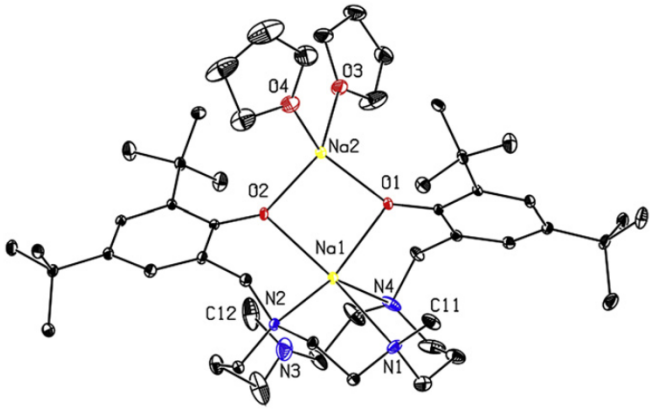

Fig. 2. Molecular structure of Na$_2$[{(Ar^{tBu2}PhO)$_2$Me$_2$Cyclam}](THF)$_2$ (**2**). Thermal ellipsoids are drawn at 40% probability level.

The other sodium cation, Na(2), lies in a distorted tetrahedron defined by two phenolate and two THF oxygen donors with angles that range from 94.4(1)° to 133.0(2)°.

The bond lengths between the cyclam nitrogens and Na(1) extend from 2.541(3) Å to 2.761(3) Å, with the shorter Na(1)–N distances involving the nitrogen atoms that are linked to the phenolate rings (N(2) and N(4)) and define two six-member metallacycles NaNC$_3$O. The Na–N(amine) distances are within the usual range reported for six-coordinate sodium complexes of cyclen derivatives (2.467(2)–2.771(2) Å) [15]. The two bridging oxygens of the phenolate groups and the two sodium ions define an almost planar four-membered Na$_2$O$_2$ ring with bonding distances to the tetra-coordinate cation much shorter than to Na(1). The Na(2)–O(Ar) bond lengths are 2.152(3) Å and 2.173(3) Å, comparable to the distances reported for {[ONNO]Na$_2$(THF)$_2$}$_2$ ([ONNO] = 1,4-bis(2-O-3,5-di-*tert*-butyl-benzyl)imidazolidine) that also displays a Na$_2$O$_2$ ring sustained by bridging phenolate rings [16]. The Na(1)–O(Ar) distances are 2.356(3) Å and 2.424(3) Å. The distances between Na(2) and the THF oxygen atoms (average 2.31 Å) are within the values usually reported for Na$^+$(THF) solvates [16–18]. The difference observed in the sodium–oxygen distances within the Na$_2$O$_2$ ring of Na$_2${(Ar^{tBu2}PhO)$_2$Me$_2$Cyclam}(THF)$_2$ (**2**) is very uncommon and must reflect that the electrons engaged in the bonding of the Na$_2$O$_2$ core are asymmetrically shared by the two metal cations. Considering the sodium–oxygen bond lengths, the structure may be described as the combination of i) a cationic fragment formed by Na(1) and six neutral donor centres bonded to

Table 1
Selected bond lengths and angles for **2a**.

Bond lengths (Å)		Angles (°)	
Na(1)–O(1)	2.356(3)	N(1)–Na(1)–N(4)	80.59(15)
Na(1)–O(2)	2.404(3)	O(1)–Na(1)–N(4)	84.72(11)
Na(2)–O(1)	2.169(3)	N(2)–Na(1)–O(2)	81.63(10)
Na(2)–O(2)	2.152(3)	Na(1)–O(1)–Na(2)	91.29(10)
Na(2)–O(3)	2.305(4)	O(1)–Na(2)–O(2)	94.37(11)
Na(1)–Na(2)	3.238(2)	O(1)–Na(2)–O(3)	101.09(13)
Na(1)–N(1)	2.640(4)	O(1)–Na(1)–O(2)	83.51(10)
Na(1)–N(2)	2.541(3)	N(1)–Na(1)–O(1)	98.73(12)
Na(1)–N(3)	2.761(6)	N(3)–Na(1)–N(2)	80.40(18)
Na(1)–N(4)	2.551(5)	O(2)–Na(1)–N(3)	98.71(15)
Na(2)–O(4)	2.324(4)	Na(1)–O(2)–Na(2)	90.44(10)
		O(3)–Na(2)–O(4)	101.57(16)

it, namely the four cyclam amines and the two oxygens O(1) and O(2), in a way that is reminiscent of Na^+ encapsulation in a neutral N_4O_2 cavity defined by a cyclen ring with two appended phenol arms [15a] and ii) an anionic fragment that is formed by the bonding of two phenolate anions to a sodium cation in which coordination sphere is completed by two THF ligands. The whole structure may thus be envisaged as composed by one $[(N_4O_2)Na(1)]^+$ and one $[Na(2)O_4]^-$ fragments that are connected to each other by the bridging phenolate oxygen atoms.

2.2. Synthesis and NMR characterization of Y(III) and Ln(III) complexes

Salt metathesis or protonolysis reactions are currently used as entries in rare-earth metal chemistry. The first approach was used in this work due to the availability of metal halides when compared to homoleptic alkyl or amido complexes. The reactions of $M_2\{(^{tBu2}PhO)_2Me_2Cyclam\}$ (M = Na, K), prepared *in situ*, with equimolar amounts of $LnCl_3(THF)_x$ (Ln = Y, La, Sm, Yb) in THF gave the corresponding $[\{(^{tBu2}PhO)_2Me_2Cyclam\}LnCl]$ complexes (Ln = Y (**4**), La (**5**), Sm (**6**), Yb (**7**)) in moderate to high yields (Scheme 2).

Compounds **4**–**6** were isolated as white solids from toluene or acetonitrile solutions. The reaction of $YbCl_3$ with one equivalent of the potassium salt **3** proceeded with a visible colour change from white to yellow occurring within seconds and **7** was isolated as a yellow crystalline solid after precipitation with *n*-hexane from a toluene extract. All $[\{(^{tBu2}PhO)_2Me_2Cyclam\}LnCl]$ compounds are readily soluble in aromatic hydrocarbons (benzene, toluene), tetrahydrofuran and acetonitrile, but the samarium complex is far less soluble in hydrocarbons than the others.

The ESI mass spectra of **4**–**7** display, in the positive ion mode, $[ML]^+$ peaks with the characteristic isotopic distributions, corresponding to the loss of Cl^-; in the negative ion mode, it was also possible to observe, for all complexes, $[MLCl_2]^-$ peaks.

The ^1H and ^{13}C NMR spectra of the yttrium compound $[\{(^{tBu2}PhO)_2Me_2Cyclam\}YCl]$ (**4**) were recorded in benzene-d_6 at room temperature and assigned on the basis of COSY, TOCSY, HSQC and HMBC experiments; the overlap of resonances did not allow its full assignment but only the distinction between the signals of the C_2 and C_3 chains of the macrocycle. The ^1H NMR spectrum shows four singlets for the ^{t}Bu groups that reveal two magnetically non-equivalent phenolate pendant arms in agreement with C_1 symmetry in solution. This was confirmed by the ^{13}C NMR, which displayed 12 signals for the 12 aromatic carbons and 10 resonances for the macrocycle. Furthermore, the two signals assigned to the quaternary carbons bonded to the oxygens of the phenolate groups (δ = 161.6 and δ = 160.7 ppm) appeared shifted to high frequencies relatively to $H_2\{(^{tBu2}PhO)_2Me_2Cyclam\}$, attesting the bonding of the phenolate groups to yttrium. The methylamine proton resonances are shifted to high- and low-frequency, respectively, in relation to the neutral ligand precursor. This behaviour is consistent with one coordinated and one non-coordinated amines, in agreement with the X-ray crystal structure of **4** (see below) [19].

The NCH_2Ar groups give rise to two AB spin systems at δ 5.64 and 2.66 ppm and δ 4.56 and 2.37 ppm with J-coupling of 13.2 Hz and 12.4 Hz, respectively. The large differences in the chemical shifts of the diastereotopic benzyl protons are striking. An analogous observation, reported for the amine bis(phenolate) complex $[Th(ONOO)Cl_2]$ (ONOO = $MeOCH_2CH_2N\{CH_2\text{-}(2\text{-}O\text{-}C_6H_2\text{-}Bu^t_2\text{-}3,5)\}_2$) was considered as resulting from an agostic interaction involving the proton directed towards the metal [20]. However the distances between the metal and H_{syn} or H_{anti} are necessarily different, $[\{(^{tBu2}PhO)_2Me_2Cyclam\}YCl]$ does not show any evidence of agostic hydrogens either in solution or in the solid state. An alternative explanation for the high shifts observed for the benzyl protons (5.64 and 4.56 ppm) may be assigned to the combined deshielding effects of the phenolate ring current and the polarization induced by the rare earth metal ion on the C–H bond pointing away from it [21].

The methylene protons of the macrocycle originate a series of complex multiplets, partially overlapped, in the range 3.66–0.74 ppm, which were ascribed to 20 resonances by HSQC experiments. The latter result, in combination with a ^1H–^1H ROESY experiment, reveals that the bonding of the cyclam to yttrium is static in the NMR time scale.

The NMR data of $[\{(^{tBu2}PhO)_2Me_2Cyclam\}LaCl]$ (**5**) in benzene-d_6 points to a C_1 symmetry in solution. The patterns of both proton and carbon spectra are closely related to those of the yttrium complex **4** except for the methyl resonances assigned to the cyclam methylamine groups. Both proton methyl resonances are shifted to high frequencies by about 0.72 and 0.32 ppm relatively to $H_2(^{tBu2}PhOH)_2Me_2Cyclam$ (**1**) what is symptomatic of their bonding to

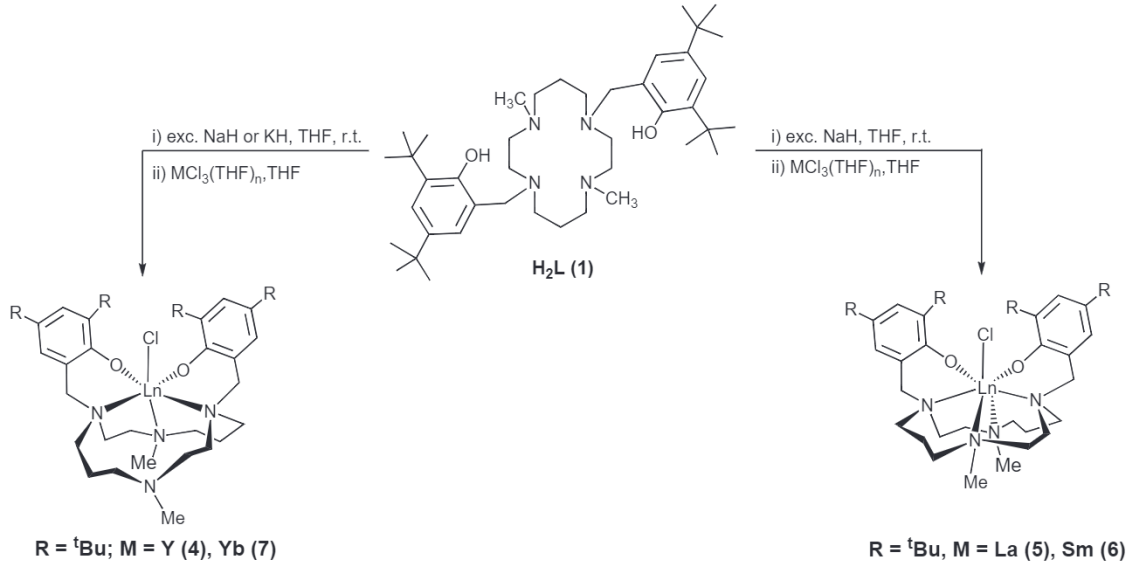

Scheme 2. Synthesis of Y(III) and Ln(III) complexes.

lanthanum and in agreement with the molecular structure depicted in Fig. 6 that shows a seven-coordinated lanthanum centre, where the ligand acts as a hexadentate donor.

The proton chemical shifts observed for the samarium complex **6** in benzene-d_6, at room temperature, are significantly shifted when compared with the diamagnetic complexes reported above but still indicative of C_1 symmetry in solution. The coordination of a ligand to a paramagnetic Ln(III) ion normally results in large chemical shifts of the ligand nuclei, with magnitudes and signs depending critically on both the nature of the lanthanide ion and the location of the nucleus relative to Ln centre [22]. In complex **6** the resonances assigned to the ^{t}Bu groups are not appreciably shifted from its usual values as they are observed as four singlets between 2.09 and 2.14 ppm. On the contrary, the resonances due to the methyl groups are strongly shifted to low frequencies (δ −1.85 and −4.01 ppm) suggesting their proximity to the metal centre and the coordination of the two cyclam methylamines to the metal. The solubility of **6** in benzene-d_8 limited the identification of other resonances and the solvent was changed to acetonitrile-d_3. In this solvent the ^{1}H NMR obtained at room temperature displayed the same resonances that were observed in benzene-d_6 and, in addition, revealed four broad resonances shifted to high frequencies (δ 12.71, 11.62, 7.08 and 6.09 ppm) assigned to the diastereotopic benzyl protons, and broad resonances corresponding to the H_{syn} and H_{anti} macrocycle protons that spread from δ 7.86 to −2.19 ppm. The complexity of the spectrum did not allow the unequivocal assignment of the macrocycle resonances but 2D NMR experiments were useful to distinguish between the [C2] and [C3] methylene chains. When an acetonitrile-d_3 solution of **6** was cooled to −30 °C all proton resonances were resolved, as shown in Fig. 3. The observation of only one set of signals for the ancillary ligand, with a pattern corresponding to C_1 symmetry complex contrasts with the solid state X-ray analysis that identified two isomers which differ from each other in the macrocycle conformations (structures **6a**-**1** and **6a**-**2**; crystals obtained from acetonitrile-d_3). The lack of duplicate signals in proton and carbon NMR spectra suggests that the two isomers interconvert in fast exchange process in the NMR time scale. The activation energy for this type of exchange is usually low [11c] and it was not possible to block the process by lowering the temperature at −30 °C.

The room temperature ^{1}H NMR spectrum of [{(^{t}Bu2PhO)$_2$Me$_2$-Cyclam}YbCl] (**7**), in benzene-d_6, displays resonances between 259 and −130 ppm, strongly shifted from the diamagnetic zone and significantly broadened, which again point to a C_1 symmetry species in solution. Four signals at 4.87, −6.27, −10.31 and −31.23 ppm

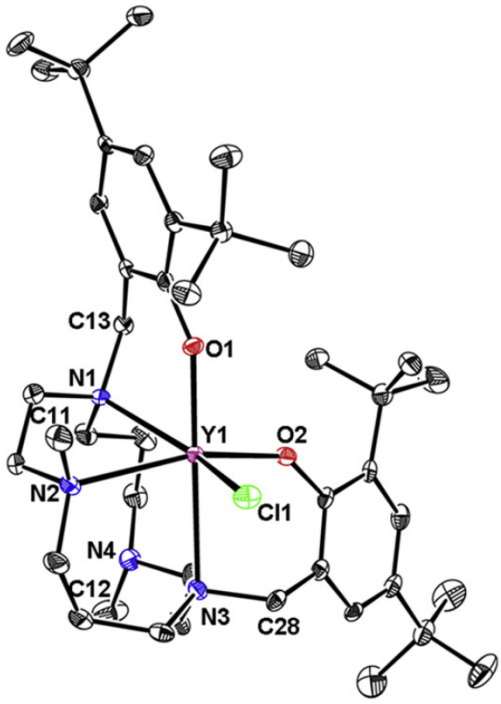

Fig. 4. Molecular structure of [Y{(Ar^{tBu2}PhO)$_2$Me$_2$Cyclam}Cl] (**4**), using 40% probability ellipsoids.

were assigned, based on the spectrum integration, to the ^{t}Bu protons of the phenolate groups and two resonances at 18.21 and −130 ppm were assigned to the N−CH_3 protons. Additionally, the proton NMR spectrum reveals twenty-eight resonances integrating to one proton each, which are attributed to four aromatic protons, four diastereotopic protons of the NCH_2Ar pendant arms and twenty H_{anti} and H_{syn} methylene protons of the cyclam ring. This pattern is in accordance with the asymmetric solid-state structure obtained for **7** (see Fig. 5).

2.3. Crystal and molecular structures of Y(III) and Ln(III) complexes

Single crystals of [{(^{t}Bu2PhO)$_2$Me$_2$Cyclam}YCl] (**4**) and [{(^{t}Bu2-PhO)$_2$Me$_2$Cyclam}YbCl] (**7**) were grown by slow diffusion of *n*-hexane in toluene solutions. Complexes **4** and **7** are isomorphous

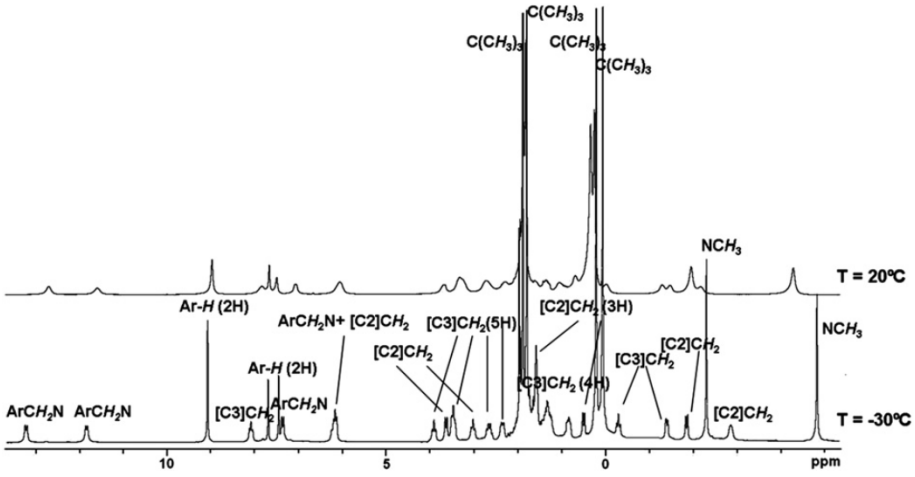

Fig. 3. ^{1}H NMR of [Sm{(Ar^{tBu2}PhO)$_2$Me$_2$Cyclam}Cl] (**6**) in acetonitrile-d_3 at 20 °C and at −30 °C.

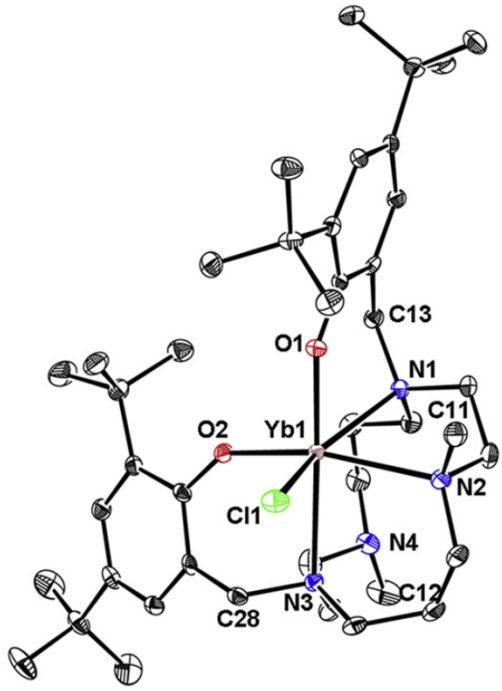

Fig. 5. Molecular structure of [Yb{(Ar^{tBu2}PhO)$_2$Me$_2$Cyclam}Cl] (**7**), using 40% probability ellipsoids.

and present monomeric structures that crystallize in the monoclinic space group $P2_1/n$ with one molecule of toluene within the lattice. Both enantiomers (RRR and SSS) are present in the centrosymmetric crystal structure. The metals are lying in six-coordinate environments defined by one chloride and the {(^{tBu2}PhO)$_2$Me$_2$Cyclam}$^{2-}$ ligand that displays κ^5-O_2N_2N' coordination mode with one NCH_3 group of the tetraazamacrocycle pointing away from the metal. ORTEP representations of **4** and **7** are depicted in Figs. 4 and 5, respectively, and selected bond lengths and angles are given in Table 2.

The complexes adopt distorted octahedral geometry with O(2), Cl(1), N(1) and N(2) defining the equatorial plane and O(1) and N(3) at the axial positions. The angles between the apical and the basal atoms vary from 74.99(9)° to 103.98(9)° in **4** and from 75.68(9)° to 104.54(9)° in **7**. The angles defined by O(1)–Ln–N(3) are 177.93(9)° and 178.19 (9)° respectively in the yttrium and the ytterbium complexes. In both compounds the two oxygen donors of the phenolate groups are mutually *cis*, as indicated by the O(1)–Y–O(2) angles of 100.23(9)° and 99.40(10)° for (**4**) and (**7**), respectively. The dihedral angles between the two phenolate planes are wide (**4**, 71.65°; **7**, 72.14°) and the aryl rings bent away from the metal, leaving a relatively open cleft for the chloride.

Table 2
Selected bond lengths (Å) and angles (°) for **4**.C_7H_8 and **7**.C_7H_8.

	4.C_7H_8	**7**.C_7H_8
Ln–O(1)	2.077(2)	2.052(2)
Ln–O(2)	2.100(2)	2.072(2)
Ln–N(1)	2.605(3)	2.581(3)
Ln–N(2)	2.539(3)	2.499(3)
Ln–N(3)	2.696(3)	2.655(3)
Ln–Cl	2.6283(10)	2.5938(10)
O(1)–Ln–O(2)	100.23(9)	99.40(10)
O(1)–Ln–N(3)	177.93(9)	178.19 (9)
O(2)–Ln–N(2)	162.24(10)	163.69(11)
N(1)–Ln–Cl(1)	152.42(7)	153.34(7)

The M–O, M–N and M–Cl bond distances for the Yb complex are 0.03–0.04 Å shorter than for Y, corresponding to the difference in the ionic radii of six coordinate Y(III) (0.90 Å) and Yb(III) (0.87 Å) [23]. The average M–O bond distances for **4** for **7** (2.088(2) Å and 2.062(2) Å, respectively) are slightly shorter than those found in the literature for acyclic amine bis(phenolate) yttrium (2.129(4)–2.161(2) Å) [1] and ytterbium complexes (2.100(3)–2.126(2) Å) [2] with the same coordination numbers, but are comparable to those found in five-coordinated complexes [(C_5Me_5)Y($OC_6H_3^tBu_2$-2,6)$_2$] [24] and [(MBMP)Yb(μ-Cl)(THF)$_2$]$_2$ (MBMP = CH_2(1-O-4-Me-6-^{t}Bu–C_6H_2)$_2$) [2d]. The metal–nitrogen distances in the equatorial plane are slightly shorter (Y: 2.605(3) and 2.539(3) Å; Yb: 2.581(3) and 2.499(3) Å) than the apical M–N distances (Y–N(3): 2.696(3) Å; Yb–N(3): 2.655(3) Å). In average M–N bond distances for **4** and for **7** compared with the values reported for acyclic diamine bis(phenolate) yttrium (2.520(5)–2.614(3) Å) [1] and ytterbium (2.476(3)–2.530(3) Å) complexes [1i,–] respectively, and with distances found in six-coordinate triazacyclononane derived metal complexes, namely [{Me_2-tacn(SiMe$_2$)NR}Y(CH_2SiMe_3)$_2$] (R = N^{t}Bu, 2.602(3) Å; R = N^{i}Bu, 2.597(8) Å) [25] and [Ln{($SiMe_2NPh$)$_3$-tacn}] (Y, 2.517(8) Å; Yb, 2.503(13) Å) [26]. The M–N(4) distances of 4.727(3) Å in **4** and 4.717(3) Å in **7** reveal that N(4) is not coordinated to the metal centres and confirm the κ^5-O_2N_2N' bonding mode of the ancillary ligand. The M–Cl bond lengths are within the ranges usually reported [1j,12,27].

Crystals of [{(^{tBu2}PhO)$_2$Me$_2$Cyclam}LaCl], **5**, suitable for X-ray structure determination were grown by slow diffusion of *n*-hexane in a toluene solution and single crystals of [{(^{tBu2}PhO)$_2$Me$_2$Cyclam}SmCl], **6**, were obtained from concentrated acetonitrile-d_3 (**6a**) and benzene-d_6 (**6b**) solutions. In crystals of **5** and **6b** the enantiomeric pairs (RRRR) and (SSSS) are both present in the centrosymmetric crystals. For **6a** there are two different isomers that display different macrocycle conformations in the asymmetric unit (**6a-1** and **6a-2**). The overall coordination of lanthanum and samarium in **5** and **6b** are comparable and thus the data for **6b** are only presented in Supplementary data. ORTEP diagrams of **5** and **6a-2** are displayed in Figs. 6 and 7, respectively. Relevant distances and angles for both compounds are listed in Table 3.

Complexes **5** and **6** present monomeric seven-coordinated structures in the solid state where the ancillary ligand binds through the $O_2N_2N'_2$ donor set and the seventh position is occupied by one chloride, defining distorted mono-capped trigonal prisms. In **5** (Fig. 6b) and **6a-1** (see Supplementary data, Fig. S3) the chloride ligand occupies one of the vertices of the prism while in **6a-2** is capping a rectangular face defined by N(6), N(7), O(3) and O(4) (Fig. 7b). In **6a-1** the face defined by O(1), N(2), N(3) and Cl(1) is capped by O(2). The four nitrogen atoms of the macrocycle ring are nearly co-planar in all structures and define one of the non-capped faces of the prism, with the metal centre sitting 1.582 Å in **5**, 1.518 Å in **6a-1** and 1.386 Å in **6a-2** above the average plane. The other non-capped quadrangular faces are defined by the O(1), Cl(1), N(1), N(4) in **5** and **6a-1**, and by O(3), O(4), N(5), N(8) in **6a-2**, with a deviation from planarity smaller than 0.19 Å. The dihedral angles between the trigonal faces defined by O(1)–N(1)–N(2) and Cl(1)–N(4)–N(3) in **5** and **6a-1**, and O(3)–N(5)–N(6) and O(4)–N(8)–N(7) in **6a-2**, are 2.84°, 4.19° and 12.03°, respectively. Analogous distortions of the polyhedron geometries have also been found in **4** and **7** and are likely due to the constraints imposed by the macrocycle ligand. The distortions are less pronounced in the La(III) complex probably due to its larger ionic radius in comparison with that of Sm(III) [23].

The oxygens of the phenolate groups are mutually *cis*, with O(1)–Ln–O(2) angles of 97.62(11)° and 95.26(8)° in **5** and **6a-1**, respectively. In **6a-2** the O(3)–Ln–O(4) angle is 96.15(9)°. The dihedral angles between the phenolate planes are 8.7° in **5**, 25.8° in **6a-1** and 66.1° in **6a-2**. In all structures the ^{t}Bu substituents and aryl rings are

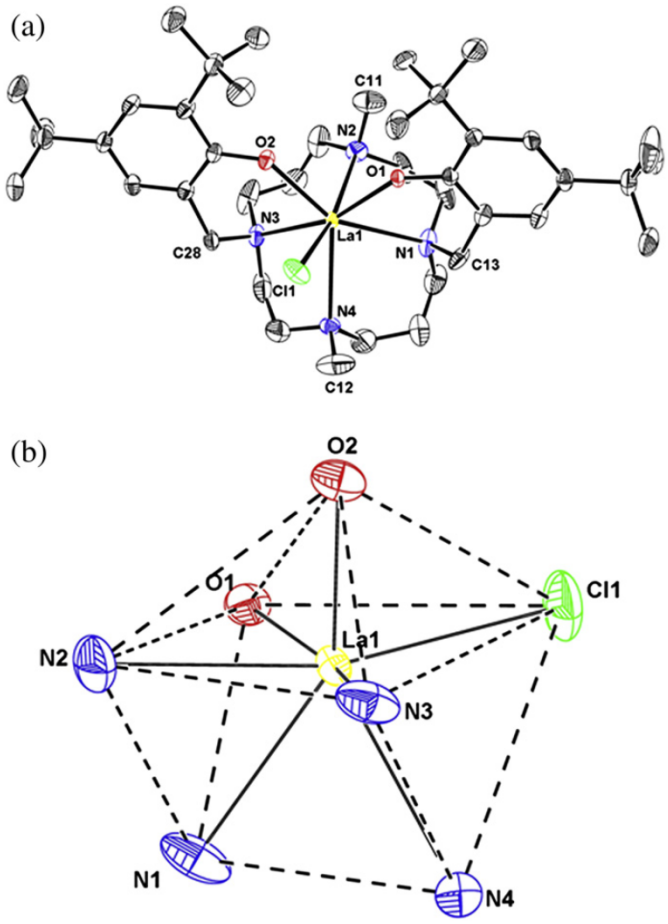

Fig. 6. (a) Molecular structure of [La{(Ar^{tBu2}PhO)$_2$Me$_2$Cyclam}Cl] (**5**). Thermal ellipsoids are drawn at 40% probability level. (b) View of the mono-capped trigonal prism coordination polyhedron of **5**.

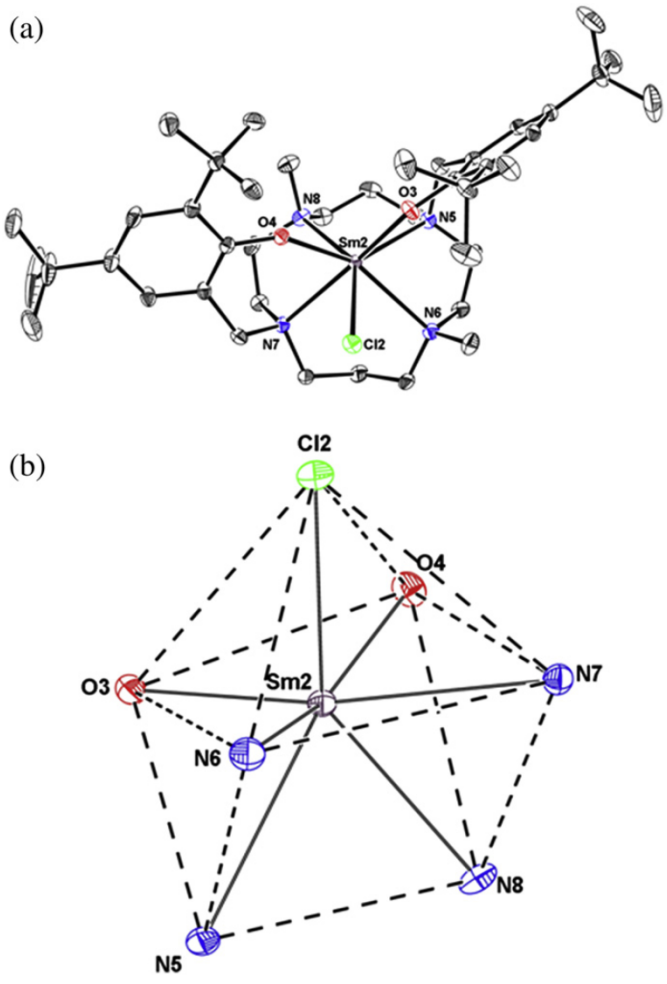

Fig. 7. (a) Molecular structure of [Sm{(Ar^{tBu2}PhO)$_2$Me$_2$Cyclam}Cl] (**6a-2**). Thermal ellipsoids are drawn at 40% probability level. (b) View of the mono-capped trigonal prism coordination polyhedron of **6a-2**.

slightly bent away from the metal and the chloride is located in the cleft between phenolate groups. The average La–O(Ar) distance (2.268(3) Å) is comparable with those of six-coordinate lanthanum complexes [La(^{tBu2}O$_2$NO){N(SiMe$_2$H)$_2$}(THF)] (ONOO = MeOCH$_2$-CH$_2$N{CH$_2$-(2-O–C$_6$H$_2$–^{t}Bu$_2$-3,5)}$_2$, av. 2.272(3) Å) [1c], [La(ONNO)]{N(SiMe$_3$)$_2$}(THF) ([ONNO] = 1,4-bis(2-O-3,5-di-tert-butylbenzyl)-imidazolidine, 2.258(6) Å) [2d] and [La(^{tBu2}O$_2$NN^{py})(μ-Cl)(py)]$_2$ ([^{tBu2}O$_2$NN^{py}] = (2-C$_5$H$_4$N)CH$_2$N{2-*O*–C$_6$H$_2$–^{t}Bu$_2$-3,5}$_2$, 2.274(4) Å) [1g]. The average Sm–O bond lengths in **6a-1** (2.194(2) Å) and **6a-2** (2.170(2) Å) are comparable with those found in the lanthanum analogue if the difference of ionic radii is considered, and to Sm–O bond lengths reported for [Sm(^{tBu2}O$_2$NN^{Me2})Cl(DME)] (2.196(1) Å) [1j], [Sm(^{tBu2}O$_2$NN^{NMe})(OAr)(THF)$_2$] (2.212(3) Å) ([^{tBu2}O$_2$NN^{NMe}] = Me$_2$NCH$_2$CH$_2$N{CH$_2$-(2-*O*–C$_6$H$_2$–^{t}Bu$_2$-3,5)}$_2$) [2b] and [({(^{tBu}ArO)$_3$tacn}Sm)$_2$(μ,η^1,η^1-SO$_2$)] (2.206(3) Å) [10a]. In **5** the average distance between the lanthanum and the cyclam nitrogens N(1), N(2) and N(3) (2.778(4) Å) is comparable to the value reported for [La{(SiMe$_2$NPh)$_3$-tacn}(THF)] (2.751(4) Å) [26] while the La–N(4) distance (2.920(4) Å) is considerably longer. Yet N(4) points to the metal, in contrast to that observed in the yttrium and ytterbium complexes discussed above.

The two structures obtained for [Sm{(Ar^{tBu2}O)$_2$Me$_2$Cyclam}Cl] (**6**) display different samarium–nitrogen bond distances. In **6a-1** the four Sm–N bonds lengths are similar and average 2.742(3) Å, a value that is slightly longer than those found in seven-coordinate samarium complexes [Sm(O$_2^{t}$^{Bu2}NN^{Me2})ClDME] (2.654(2) Å) [12] and [Sm(O$_2^{t}$^{Bu2}NN^{Me2})(OAr)(THF)] (2.674(4) Å) [2b]. The Sm–N bonds lengths range from 2.632(3) Å to 2.827(3) Å in **6a-2**. The Ln–Cl bond distances are comparable in the three structures (2.7883(12) Å for **5**, 2.7385(9) Å for **6a-1** and 2.7339(9) Å for **6a-2**) and within the values reported for other complexes [1l,28].

Table 3
Selected bond lengths (Å) and angles (°) for **5**.C$_7$H$_8$ and **6a**.CD$_3$CN.

	5	**6a-1**		**6a-2**
Ln–O(1)	2.250(3)	2.182(2)	Ln–O(3)	2.166(2)
Ln–O(2)	2.285(3)	2.206(2)	Ln–O(4)	2.174(2)
Ln–N(1)	2.815(4)	2.729(3)	Ln–N(5)	2.827(3)
Ln–N(2)	2.789(4)	2.771(3)	Ln–N(6)	2.707(3)
Ln–N(3)	2.731(4)	2.750(3)	Ln–N(7)	2.632(3)
Ln–N(4)	2.920(4)	2.716(3)	Ln–N(8)	2.759(3)
Ln–Cl	2.7883(12)	2.7385(9)	Ln–Cl	2.7339(9)
O(1)–Ln–O(2)	97.62(11)	95.26(8))	O(3)–Ln–O(4)	96.15(9)
O(1)–Ln–N(3)	160.30(13)	168.46(9)	O(3)–Ln–N(7)	170.24(9)
O(2)–Ln–N(2)	81.93(13)	82.42(8)	O(4)–Ln–N(6)	154.67(9)
O(2)–Ln–N(1)	148.88(14)	143.39(9)	O(4)–Ln–N(5)	138.35(9)
O(2)–Ln–N(3)	71.46(12)	74.73(8)	O(4)–Ln–N(7)	76.22(9)
O(2)–Ln–Cl(1)	86.06(9)	83.23(6)	O(4)–Ln–Cl(2)	81.78(7)
O(1)–Ln–Cl(1)	89.76(9)	87.13(7)	O(3)–Ln–Cl(2)	94.64(7)
N(2)–Ln–Cl(1)	165.70(10)	165.65(6)	N(6)–Ln–Cl(2)	74.29(7)
N(1)–Sm–N(2)	65.56(9)	68.52(14)	N(5)–Ln–N(6)	66.97(9)
N(3)–Ln–N(4)	68.82(9)	67.79(13)	N(7)–Ln–N(8)	68.23(9)
O(2)–Ln–N(4)	132.01(12)	137.01(9)	O(4)–Ln–N(8)	78.94(9)
N(4)–Ln–Cl(1)	81.36(9)	79.56(6)	N(8)–Ln–Cl(2)	144.51(7)

3. Conclusions

A new dianionic cyclam-based ligand of the type $[N_4O_2]^{2-}$ and its M(III) complexes (M = Y, Yb, La, Sm) are described. The ligand precursor was obtained in high yield from cyclam by sequential functionalization of the ring nitrogen atoms with Me and 2-hydroxy-3,5-di-tert-butylbenzyl leading to a tetrasubstituted macrocycle with *trans*-Me and *trans*-(^{tBu2}PhOH) groups. Complexes of general formula [{(^{tBu2}PhO)$_2$Me$_2$Cyclam}MCl] are, to the authors' knowledge, the first examples of yttrium and lanthanide complexes with phenolate substituents appended on a saturated tetraaza-macrocycle. In the Y and Yb complexes the ligand adopts a κ^5-O_2N_2N' bonding mode with one NMe group pointing out away from the metals; the larger La and Sm ions accommodate the six ligand donor atoms and the chloride, defining capped trigonal prismatic structures. The ability of tetradentate dianionic cyclam based ligands to behave as hemilabile ligands was well establish in the chemistry of d^0 Zr(IV) complexes. The results described now show that this behaviour is extensive to Y and Ln metal complexes and, analogously to zirconium, is dictated by steric constraints. As envisaged, the combination of the cyclic tetraamine with the phenolate donors prevents ligand redistribution and dimerization. The efficient steric protection offered by the cyclam skeleton increases the robustness of [{(^{tBu2}PhO)$_2$Me$_2$Cyclam}MCl] in comparison with related compounds supported by acyclic ligands and provides well-defined mono-halide bis(phenolate) Y and Ln complexes. Preliminary reactions of the yttrium complex with alkylating reagents led to mono-alkyl complexes which are currently under study.

4. Experimental

4.1. General procedures

All reactions were carried out under inert atmosphere, using standard Schlenk techniques or in a nitrogen-filled glovebox. Tetrahydrofuran, toluene and hexane were pre-dried using 4 Å molecular sieves and distilled from sodium-benzophenone under nitrogen and degassed prior to use. Tetrahydrofuran-d_8, benzene-d_6 and toluene-d_8 were dried over sodium-benzophenone. Acetonitrile and acetonitrile-d_3 were distilled from P_2O_5 under nitrogen and maintained in contact with molecular sieves several days before use. $YCl_3(THF)_{2.5}$, $LaCl_3(THF)_{1.5}$, $SmCl_3$, $YbCl_3$ and 1,4,8,11-tetraazacyclotetradecane were prepared as previously reported [29,30]. All other reagents were commercial grade and used without further purification.

^{1}H, ^{13}C NMR spectra and 2D NMR experiments were recorded using Varian 300 MHz or Bruker AVANCE 400 or 500 MHz spectrometers. ^{1}H and ^{13}C chemical shifts were referenced internally to residual proton or carbon solvents resonances relative to tetramethylsilane (0 ppm). Electrospray ionisation mass spectrometry (ESI-MS) was performed using a Bruker HCT quadrupole ion trap mass spectrometer. Carbon, hydrogen and nitrogen analyses were performed on a CE Instruments EA1110 automatic analyser.

4.2. Synthesis and characterization data

4.2.1. H_2[(Ar^{tBu2}PhO)$_2$Me$_2$Cyclam (H_2L) (**1**)

37% aqueous formaldehyde (0.8 ml, mmol) was added to a solution of 1,8-dimethyl-1,4,8,11-tetraazacyclotetradecane (790 mg, 3.46 mmol) in methanol (20 ml). The mixture was refluxed under N_2 for 2 h and a solution of 2,4-di-tert-butylphenol (1.43 g, 6.92 mmol) in methanol (10 ml) was then added and refluxed overnight. The white precipitate formed was isolated by filtration, washed with methanol and dried under vacuum. Yield: 85% (1.94 g, 2.94 mmol). Crystals suitable for X-ray diffraction analysis were grown from a diluted solution of **1** in acetonitrile. *m*/*z* (ESI-MS): 665.5 $[H_2L + H]^+$ (calc. 665.57). Calc. for $C_{42}H_{72}O_2N_4$: C, 75.85; H, 10.91; N, 8.42. Found C, 75.22, H, 10.98, N, 8.45. ^{1}H NMR (C_6D_6, 300 MHz, 295 K): δ (ppm) 10.00 (s, 2H, Ar–O*H*), 7.51 (d, $^4J_{HH}$ = 2.4 Hz, 2H, Ar–*H*), 7.01 (d, $^4J_{HH}$ = 2.4 Hz, 2H, Ar–*H*), 3.90 (br, 2H, ArC*H*$_2$N), 3.35 (br, 2H, [C2]NC*H*$_2$), 3.08 (br, 2H, [C3]NC*H*$_2$), 2.54 (br, overlapping, 2H + 2H + 2H, [C2]NC*H*$_2$, [C3]NC*H*$_2$ and ArC*H*$_2$N), 2.05 (br, overlapping, 2H + 2H, [C3]NC*H*$_2$ and $CH_2CH_2CH_2$), 1.93 (s, 6H, NC*H*$_3$), 1.89 (br, 2H, [C2]NC*H*$_2$), 1.70 (s, 18H, C(C*H*$_3$)$_3$), 1.65 (2H, br, [C2]NC*H*$_2$), 1.38 (s, 18H, C(C*H*$_3$)$_3$), 1.34 (br, 2H, $CH_2CH_2CH_2$), 1.08 (br, 2H, [C3]NC*H*$_2$). ^{13}C NMR (C_6D_6, 100 MHz, 295 K): δ (ppm) 154.3 (ArC–O), 139.9 (ArC), 135.6 (ArC), 125.5 (ArC–H), 123.6 (ipso-ArC), 122.9 (ArC–H), 55.6 (NCH_2Ar), 54.7 ([C2]NCH_2), 51.4 ([C3]NCH_2), 51.2 ([C3]NCH_2), 48.4 ([C2]NCH_2), 43.1(NCH_3), 35.4 (*C*(CH$_3$)$_3$), 34.3 (*C*(CH$_3$)$_3$), 32.1 (C(*C*H$_3$)$_3$), 30.2 (C(*C*H$_3$)$_3$), 24.7 ($CH_2CH_2CH_2$).

4.2.2. Na_2[(Ar^{tBu2}PhO)$_2$Me$_2$Cyclam](THF)$_2$ (**2**)

A suspension of NaH (55 mg, 2.29 mmol) in THF (10 ml) was added to a stirred solution of H_2[(Ar^{tBu2}O)$_2$Cyclam] (435 mg, 0.654 mmol) in THF (20 ml). The resulting mixture was stirred overnight at room temperature and then centrifuged. The solvent of the supernatant was removed under vacuum and the alkali salt **2** was obtained in quantitative yield as a white powder. Colourless prismatic crystals suitable for X-ray crystallographic analysis of compound **2** were obtained from a concentrated solution in THF stored at −20 °C for several days. Anal. Calc. for $C_{50}H_{86}O_4N_4Na_2$: C, 70.38; H, 10.16; N, 6.57. Found C, 69.14, H, 8.74, N, 6.47. ^{1}H NMR (THF-d_8, 300 MHz, 295 K): δ (ppm) 7.07 (d, $^4J_{HH}$ = 2.4 Hz, 2H, Ar–*H*), 6.83 (br, 2H, Ar–*H*), 4.21 (br, 2H, ArC*H*$_2$N), 3.02–2.59 (br, overlapping, 2H + 2H, NC*H*$_2$, 2H, ArC*H*$_2$N), 2.44 (br, 6H, NC*H*$_2$), 1.93 (br, 2H + 2H, NC*H*$_2$), 1.81 (br, 3H + 2H, NC*H*$_3$ + NC*H*$_2$), 1.44 (s, 18H, C(C*H*$_3$)$_3$), 1.23 (s, 18H, C(C*H*$_3$)$_3$), 1.09 (br, 2H, $CH_2CH_2CH_2$), 0.94 (br, 2H, $CH_2CH_2CH_2$). ^{13}C {^{1}H} NMR (THF-d_8, 75.4 MHz, 295 K): δ (ppm) 168.6 (ArC–O), 135.5 (ArC), 129.9 (ArC), 127.7 (ArC–H), 125.9 (ArC–H), 123.4 (ArC–H), 68.2 (THF), 67.4 (ArCH$_2$N), 65.9 (br, *C*H$_2$), 59.7 (br, *C*H$_2$), 58.0 (br, *C*H$_2$), 54.6 (br, *C*H$_2$), 49.9 (br, *C*H$_2$), 43.6 (NCH_3), 35.9 (*C*(CH$_3$)$_3$), 34.2 (*C*(CH$_3$)$_3$), 32.6 (C(*C*H$_3$)$_3$), 31.2 (C(*C*H$_3$)$_3$), 26.5 (br, $CH_2CH_2CH_2$), 26.4 (THF).

4.2.3. K_2[(Ar^{tBu2}PhO)$_2$Me$_2$Cyclam](THF)$_2$ (**3**)

This compound was prepared from the precursor **1** and KH by an identical procedure to that employed for compound **2**. Compound **3** was obtained in a quantitative yield and as a white solid. Anal. Calc. for $C_{50}H_{86}O_4N_4K_2$: C, 67.82; H, 9.79; N, 6.33. Found C, 66.57, H, 8.88, N, 6.50. ^{1}H NMR (THF-d_8, 300 MHz, 295 K): δ (ppm) 7.00 (d, $^4J_{HH}$ = 2.7 Hz, 2H, Ar–H), 6.82 (br, $^4J_{HH}$ = 2.7 Hz, 2H, Ar–*H*), 3.90 (br, 2H, C*H*$_2$), 2.86–2.30 (br, 10H, C*H*$_2$), 2.28–1.97 (br, 6H, CH$_2$), 1.77 (6H, NC*H*$_3$), 1.43 (s, 18H, C(C*H*$_3$)$_3$), (2H, br), 1.23 (18H, C(C*H*$_3$)$_3$), 1.30–1.10 (br, 4H, $CH_2CH_2CH_2$). ^{13}C {1H} NMR (THF-d_8, 75.4 MHz, 295 K): δ (ppm) 168.1 (ArC–O), 135.2 (ArC), 128.4 (ArC), 124.9 (ArC), 122.7 (ArC), 68.2 (THF), 63.6 (br, ArCH$_2$N), 61.8 (br, *C*H$_2$), 58.6 (br, *C*H$_2$), 56.9 (br, *C*H$_2$), 42.5 (br, NCH$_3$), 35.6 (*C*(CH$_3$)$_3$), 34.2 (*C*(CH$_3$)$_3$), 32.6 (C(*C*H$_3$)$_3$), 30.5 (C(*C*H$_3$)$_3$), 27.6 ($CH_2CH_2CH_2$), 26.4 (THF).

4.2.4. [Y{(Ar^{tBu2}PhO)$_2$Me$_2$Cyclam}Cl] (**4**)

A solution of H_2L (0.435 g, 0.654 mmol) in THF (10 ml) was added to a suspension of NaH (0.055 g, 2.29 mmol) in the same solvent (5 ml) and stirred overnight at room temperature. The mixture was centrifuged and the colourless solution of Na_2L was slowly added to a suspension of $YCl_3(THF)_3$ (0.270 g, 0.655 mmol) in THF (20 ml). The mixture was stirred overnight at room temperature and the NaCl formed was discharged after centrifugation. The solvent was removed under reduced pressure. The white solid obtained was extracted in toluene and *n*-hexane was added to the solution. A white precipitate was isolated by centrifugation and

Table 4
Experimental crystal data and structure refinement parameters for compounds **1** and **2**.

	1	**2**
Empirical formula	$C_{42}H_{72}N_4O_2$	$C_{50}H_{86}N_4Na_2O_4$
Formula weight	665.04	853.21
Cryst system	Orthorhombic	Monoclinic
Space group	Pbca	P21/*c*
a [Å]	18.1488(10)	32.377(3)
b [Å]	8.2358(4)	14.8305(15)
c [Å]	27.1280(15)	22.299(2)
α [°]	90	90
β [°]	90	106.357(6)
γ [°]	90	90
V [Å^3]	4054.8(4)	10,273.7(18)
Z	4	8
Calculate density (mg/m^{-3})	1.089	1.103
μ (mm^{-1})	0.066	0.083
T_{min}/T_{max}	0.9869/0.9960	0.9795/0.9967
F(000)	1472	3744
θ_{max} (°)	25.03	25.03
Reflections collected	15,375	131,915
Unique reflections collected (R_{int})	3567 (0.0875)	18,060 (0.1269)
R_1 [$I > 2\sigma(I)$]	0.0506	0.0866
wR2 (all data)	0.1145	0.2679
Parameters	217	1118
Goodness-of-fit on F2	0.917	1.014
Largest diff. peak, hole/*e* Å^{-3}	0.176, −0.212	1.061, −0.792

dried in vacuum to give compound **4** in 45% yield (0.232 g, 0.295 mmol). Crystals suitable for X-ray diffraction analysis were obtained by slow diffusion of n-hexane into a saturated toluene solution of 4. *m/z* (ESI-MS): 751.6 $[YL]^+$ (calc. 751.46), 821.8 $[YLCl_2]^-$ (calc. 821.39). Calc. for $C_{42}H_{70}ClN_4O_2Y.1.5C_7H_8$: C, 68.14, H, 8.87, N, 6.06. Found C, 69.08, H, 8.33, N, 6.68. ^{1}H NMR (C_6D_6, 400.1 MHz, 295 K): δ (ppm) 7.66 (d, 1H, $^4J_{HH}$ = 2.1 Hz, Ar−*H*), 7.51 (1H, Ar−H), 7.05 (1H, Ar−H), 6.95 (1H, Ar−H), 5.64 (d, 1H, J_{HH} = 13.2 Hz, ArC*H*$_2$N), 4.56 (d, 1H, J_{HH} = 12.4 Hz, ArC*H*$_2$N) 3.66 (m, 1H, [C3]NC*H*$_2$), 3.56 (1H, [C3]NC*H*$_2$), 3.04 (t, 1H, [C2]NC*H*$_2$), 2.88 (t, 1H, [C3]NC*H*$_2$), 2.66 (d, 1H, J_{HH} = 12.4 Hz, ArC*H*$_2$N), 2.51−2.37 (m, overlapping, 4H total, 1H, ArC*H*$_2$N and 1H + 1H + 1H, [C2]NC*H*$_2$), 2.09 (s, 3H, NC*H*$_3$), 2.04 (br, 1H, [C2]NC*H*$_2$), 1.99 (br, 1H, $CH_2CH_2CH_2$), 1.92 (s, 9H, C(C*H*$_3$)$_3$), 1.85 (s, 3H, NC*H*$_3$), 1.74 (br, 3H total, 1H + 2H, [C3]NC*H*$_2$), 1.64 (s, 9H, C(C*H*$_3$)$_3$), 1.45 (s, 9H, C(C*H*$_3$)$_3$), 1.44 (overlapping, 1H + 9H, C(C*H*$_3$)$_3$ and [C3]NC*H*$_2$), 1.40−1.25 (br, overlapping, 4H total, 1H, [C2]NC*H*$_2$, 1H, [C3]NC*H*$_2$, 1H + 1H, $CH_2CH_2CH_2$), 1.20 (d, 1H, [C2]NC*H*$_2$), 0.85 (1H, br, $CH_2CH_2CH_2$), 0.74 (d, 13.2 Hz, 1H, [C2]NC*H*$_2$). ^{13}C {^{1}H} NMR (C_6D_6, 100.6 MHz, 295 K): δ (ppm) 161.6 (Ar*C*−O), 160.7 (Ar*C*−O), 137.9 (Ar*C*), 137.8 (Ar*C*), 137.5 (Ar*C*), 136.1 (Ar*C*), 126.7 (*ipso*-Ar*C*), 125.4 (Ar*C*−H), 125.0 (Ar*C*−H), 124.7 (Ar*C*−H), 123.8 (Ar*C*−H), 123.0 (*ipso*-Ar*C*), 67.6 (Ar*C*H$_2$N), 62.8 ([C2]NCH$_2$), 62.5 (ArCH$_2$N), 61.8 ([C3]NCH$_2$), 60.2 ([C3]NCH$_2$), 54.3 ([C3]NCH$_2$), 53.3 ([C3]NCH$_2$), 52.6 ([C2]NCH$_2$), 51.2 ([C2]NCH$_2$), 51.1 ([C2]NCH$_2$), 45.9 (NCH$_3$), 44.4 (NCH$_3$), 35.7 (*C*(CH$_3$)$_3$), 35.4 (*C*(CH$_3$)$_3$), 34.32 (*C*(CH$_3$)$_3$), 34.29 (*C*(CH$_3$)$_3$), 32.3 (C(*C*H$_3$)$_3$), 34.3 (C(*C*H$_3$)$_3$), 30.5 (C(*C*H$_3$)$_3$), 30.4 (C(*C*H$_3$)$_3$), 25.5 ($CH_2CH_2CH_2$), 22.9 ($CH_2CH_2CH_2$).

4.2.5. [La{(^{tBu2}PhO)$_2$Me$_2$Cyclam}Cl] (**5**)

A solution of H_2L (0.350 g, 0.526 mmol) in THF (10 ml) was added to a suspension of NaH (0.045 g, 1.87 mmol) in the same solvent (5 ml) and stirred overnight at room temperature. The mixture was centrifuged and the colourless solution of Na_2L was slowly added to a suspension of $LaCl_3(THF)_{1.5}$ (0.186 g, 0.526 mmol) in THF. After stirring overnight at room temperature, the NaCl formed was discarded by centrifugation and the colourless solution was separated and evaporated to dryness. The solid obtained was extracted in toluene and upon filtration the solvent was evaporated in vacuum. The solid residue was further extracted in acetonitrile followed by evaporation of the volatiles under reduced pressure to yield **5** as a white crystalline powder, in 61% yield (0.268 g, 0.320 mmol).

Colourless crystals of [La{(Ar^{tBu2}O)$_2$Me$_2$Cyclam}Cl] (**5**) suitable for X-ray diffraction analysis were grown from slow diffusion of *n*-hexane into a concentrated solution of 5 in toluene. *m/z* (ESI-MS): 801.5 $[LaL]^+$ (calc. 801.46), 871.4 $[LaLCl_2]^-$ (calc. 871.39). Calc. for $C_{42}H_{70}ClN_4O_2La$: C, 60.24, H, 8.43, N, 6.69. Found C, 59.84, H, 9.08, N, 6.73.

^{1}H NMR (C_6D_6, 300.1 MHz, 295 K): δ (ppm) 7.65 (1H, d, $^4J_{HH}$ = 2.4 Hz, Ar−H), 7.62 (d, $^4J_{HH}$ = 2.4 Hz, 1H, Ar−H), 7.05 (d, $^4J_{HH}$ = 2.6 Hz, 1H, Ar−H), 6.99 (d, $^4J_{HH}$ = 2.6 Hz, 1H, Ar−H), 5.28 (d, $^2J_{H-H}$ = 12.4 Hz, 1H, ArC*H*$_2$N), 3.90 (d, $^2J_{HH}$ = 12.6 Hz, 1H, ArC*H*$_2$N),

Table 5
Experimental crystal data and structure refinement parameters for compounds **4**–**7**.

	4.C_7H_8 (Ln = Y)	**5**.0.5(C_7H_8) (Ln = La)	**6a**.0.5(CD_3CN) (Ln = Sm)	**6b**.(C_6D_6) (Ln = Sm)	**7**.C_7H_8 (Ln = Yb)
Empirical formula	$C_{49}H_{78}ClN_4O_2Y$	$C_{91}H_{147}Cl_2La_2N_8O_4$	$C_{86}H_{143}Cl_2N_9O_4Sm_2$	$C_{48}H_{76}ClN_4O_2Sm$	$C_{49}H_{78}ClN_4O_2Yb$
Formula weight	879.51	1765.89	1738.69	926.93	963.64
Cryst system	Monoclinic	Monoclinic	Triclinic	Monoclinic	Monoclinic
Space group	P2$_1$/*n*	P2$_1$/*n*	P-1	P 2$_1$/*c*	P2$_1$/*n*
a [Å]	21.1325(6)	12.1521(3)	15.5587(5)	15.8316(3)	21.0770(7)
b [Å]	8.7207(2)	15.0234(3)	18.0637(6)	14.8137(3)	8.7264(3)
c [Å]	27.9236(10)	26.2133(5)	18.3416(6)	23.9510(5)	27.8876 (9)
α [°]	90	90	84.030(2)	90.00	90
β [°]	94.205(2)	91.2270(10)	69.529(2)	104.9750(10)	94.5670(10)
γ [°]	90	90	68.807(2)	90.00	90
V [Å^3]	5132.2(3)	4784.56(18)	4501.2(3)	426.33(19)	5113.0(3)
Z	4	2	2	4	4
Calculate density (mg/m^{-3})	1.138	1.226	1.283	1.135	1.252
μ (mm^{-1})	1.226	0.986	1.401	1.166	1.919
T_{min}/T_{max}	0.7099/0.9759	0.7564/0.8123	0.7865/0.8726	0.7672/0.8002	0.6559/0.9272
F(000)	1888	1858	1824	1948	2012
θ_{max} (°)	25.03	25.03	25.68	25.03	25.68
Reflections collected	37,375	27,688	45,077	43,795	36,255
Unique reflections collected (R_{int})	9026 (0.0951)	8426 (0.0399)	17,015 (0.0516)	9548 (0.1070)	9708 (0.0621)
R_1 [$I > 2\sigma(I)$]	0.0524	0.0491	0.0361	0.0901	0.0349
wR2 (all data)	0.1204	0.1180	0.0847	0.1980	0.0758
Parameters	529	497	943	518	529
Goodness-of-fit on F2	0.948	1.054	1.002	1.226	0.981
Largest diff. peak, hole/*e* Å^{-3}	0.689, −0.453	1.426, −0.753	0.981, −0.601	2.723, −5.136	0.718, −0.595

3.48 (t, 1H, [C2]NCH_2), 3.14 (t, 1H, [C2]NCH_2), 2.93 (br, 2H, [C2]NCH_2 + [C3]NCH_2), 2.84 (br, 2H, [C3]NCH_2), 2.66 (s, 3H, NCH_3), 2.60–2.59 (m, 2H, [C2]NCH_2 + ArCH_2N), 2.55 (d, $^2J_{HH}$ = 12.4 Hz, 1H, ArCH_2N), 2.25 (3H, NCH_3), 1.94 (br, 1H, [C3]NCH_2), 1.90 (s, 9H, C(CH_3)$_3$), 1.88 (s, 9H, C(CH_3)$_3$), 1.83–1.59 (br, 6H, 2X[C2]NCH_2 + 3X[C3]NCH_2 + CH$_2$CH_2CH$_2$), 1.57 (br, 1H, [C3]NCH_2), 1.50 (s, 9H, C(CH_3)$_3$), 1.49 (s, 9H, C(CH_3)$_3$), 1.22 (br, 1H, [C2]NCH_2), 1.19 (br, 1H, CH$_2$CH_2CH$_2$), 1.11 (d, 1H, CH$_2$CH_2CH$_2$), 0.96 (br, overlapping, 2H, [C2]NCH_2 + CH$_2$CH_2CH$_2$).

^{13}C {^{1}H} NMR (C_6D_6, 75.4 MHz, 295 K): δ (ppm) 163.7 (ArC–O), 162.8 (ArC–O), 137.1 (ArC), 136.6 (ArC), 136.3 (ArC), 135.8 (ArC), 126.0 (ArC–H), 125.8 (ArC–H), 124.6 (ArC), 124.5 (ArC–H), 124.2 (ArC–H), 63.8 (ArCH$_2$N), 62.4 (ArCH$_2$N), 62.5 ([C3]NCH$_2$), 62.4 ([C3]NCH$_2$), 60.0 ([C3]NCH$_2$), 56.9 (2C, [C2]NCH$_2$ + [C2]NCH$_2$), 56.1 ([C2]NCH$_2$), 55.3([C2]NCH$_2$), 51.1 (NCH$_2$), 47.7 (NCH$_3$), 45.8 (NCH$_3$), 35.9 (C(CH$_3$)$_3$), 35.8 (C(CH$_3$)$_3$), 34.3 (C(CH$_3$)$_3$), 34.2 (C(CH$_3$)$_3$), 32.5 (C(CH$_3$)$_3$), 32.4 (C(CH$_3$)$_3$), 31.7 (C(CH$_3$)$_3$), 31.2 (C(CH$_3$)$_3$), 24.9 (CH$_2$CH$_2$CH$_2$), 21.6 (CH$_2$CH$_2$CH$_2$).

4.2.6. [Sm{(Ar^{tBu2}PhO)$_2$Me$_2$Cyclam}Cl] (**6**)

A solution of H_2L (0.400 g, 0.601 mmol) in THF (10 ml) was added to a suspension of NaH (0.051 g, 2.10 mmol) in THF (5 ml) and stirred overnight at room temperature. The mixture was centrifuged and the colourless solution of Na_2L was slowly added to a suspension of $SmCl_3$ (0.155 g, 0.603 mmol) in THF. After stirring overnight, the NaCl formed was discarded by centrifugation and the pale yellow solution was filtered off and evaporated to dryness. The residue was extracted in acetonitrile. The solvent was removed under vacuum to yield compound **6** as a pale yellow powder, in 87% yield (445 mg, 0.524 mmol). Colourless crystals suitable for X-ray diffraction analysis were obtained from a benzene-d_6 or acetonitrile-d_3 solution of compound **6** at room temperature. *m/z* (ESI-MS): 814.6 [SmL]$^+$ (calc. 814.47), 886.5 [SmLCl$_2$]$^-$ (calc. 886.41). Calc. for $C_{42}H_{70}ClN_4O_2Sm$: C, 59.43, H, 8.31, N, 6.60. Found C, 59.20, H, 8.11, N, 6.86. ^{1}H NMR (CD$_3$CN, 300.1 MHz, 295 K): δ 12.71 (br, 1H, ArCH_2N), 11.62 (br, 1H, ArCH_2N), 8.97 (s, 2H, Ar–H), 7.86 (br, 1H, [C3]NCH_2), 7.66 (s, 1H, Ar–H), 7.49 (s, 1H, Ar–H), 7.08 (br, 1H, ArCH_2N), 6.09 (br, 2H, ArCH_2N + [C2]NCH_2), 3.69 (1H, [C3]NCH_2), 3.33 (3H, 2H [C3]NCH_2 + 1H [C2]NCH_2), 2.72 (br, 2H, CH$_2$CH_2CH$_2$ + [C2]NCH_2), 2.28 (br, 1H, CH$_2$CH_2CH$_2$), 1.87 (9H + 1H, C(CH_3)$_3$ + [C2]CH$_2$), 1.81 (9H + 1H, C(CH$_3$)$_3$ + [C2]NCH_2), 1.59 (br, 1H, [C3]NCH_2), 1.39 (br, 1H, CH$_2$CH_2CH$_2$), 1.04 (br, 1H, CH$_2$CH_2CH$_2$), 0.69 (br, 1H, [C3]NCH_2), 0.33 (s, 9H + 1H, C(CH_3)$_3$ + [C2]NCH_2), 0.24 (s, 9H, C(CH$_3$)$_3$), −0.04 (br, 1H, [C3]NCH_2), −1.29 (1H, [C3]CH_2), −1.48 (1H, [C2]NCH_2), −1.96 (br, 3H, NCH_3), −2.19 (1H, [C2]NCH_2), −4.30 (br, 3H, NCH_3). ^{13}C {^{1}H} NMR (CD$_3$CN, 75.5 K, 295 K): δ (ppm) 171.1 (ArC–O), 164.8 (ArC–O), 138.6 (ArC), 137.6 (ArC), 133.3 (ArC), 133.0 (ArC), 131.6 (ArC), 130.8 (ArC), 130.1 (ArC–H), 129.6 (ArC–H), 125.1 (ArC–H), 124.7 (ArC–H), 78.0 (ArCH$_2$N), 75.2 (ArCH$_2$N), 65.7 ([C3]NCH$_2$), 64.3 (2C overlapping, [C3]NCH$_2$), 60.6 ([C2]NCH$_2$), 58.1 ([C2]NCH$_2$), 57.6 ([C2]NCH$_2$), 57.2 ([C3]NCH$_2$), 53.5 ([C2]NCH$_2$), 43.3 (NCH$_3$), 43.0 (NCH$_3$), 36.0 (C(CH$_3$)$_3$), 35.445 (C(CH$_3$)$_3$), 32.5 (C(CH$_3$)$_3$), 30.6 (C(CH$_3$)$_3$), 30.1 (C(CH$_3$)$_3$), 26.6 (CH$_2$CH$_2$CH$_2$), 21.4 (CH$_2$CH$_2$CH$_2$).

4.2.7. [Yb{(Ar^{tBu2}PhO)$_2$Me$_2$Cyclam}Cl] (**7**)

A solution of H_2L (0.300 g, 0.451 mmol) in THF (10 ml) was added to a suspension of KH (0.064 g, 1.58 mmol) in THF (5 ml), and the mixture was stirred overnight at room temperature. The mixture was centrifuged and the colourless solution of K_2L was slowly added to a white suspension of $YbCl_3$ (0.126 g, 0.451 mmol) in THF. The reaction proceeded with a visible colour change of white to deep yellow. After stirring overnight at room temperature, the KCl formed was discarded by centrifugation and the volatiles of the separated solution were removed under reduced pressure.

The yellow solid obtained was extracted in toluene, filtered, and *n*-hexane was added to the solution. A yellow precipitate was isolated by centrifugation and dried to give **7**, in 43% yield (0.170 g, 0.195 mmol). Crystals of **7** suitable for X-ray diffraction analysis were grown over few days by slow diffusion of *n*-hexane into a concentrated toluene solution of 7. *m/z* (ESI-MS): 836.5 [YbL]$^+$ (calc. 836.49), 906.4 [YbLCl$_2$]$^-$ (calc. 906.43).Calc. for $C_{42}H_{70}ClN_4O_2Yb$: C, 57.88, H, 8.10, N, 6.43; Found C, 57.11, H, 7.44, N, 6.08. ^{1}H NMR (C_6D_6, 300.1 MHz, 295 K): δ (ppm) 258.9 (1H), 191.3 (1H), 135.986 (1H), 100.90 (1H), 96.9 (1H), 74.4 (1H), 63.2 (1H), 60.57 (1H), 58.74 (1H), 39.86 (1H), 19.41 (1H), 18.21 (3H, NCH_3), 4.87 (9H, C(CH_3)$_3$), −6.27 (9H, C(CH_3)$_3$), −9.40 (1H), −10.00 (1H), −10.31 (9H, C(CH$_3$)$_3$), −13.37 (1H), −13.94 (1H), −16.74 (1H), −27.97 (1H), −30.29 (1H), −30.64 (1H), −31.23 (9H, C(CH_3)$_3$), −41.17 (1H), −41.86 (1H), −48.83 (1H), −51.05 (1H), −54.70 (1H), −57.34 (1H), −67.67 (1H), −71.42 (1H), −75.51 (1H), −130.0 (3H, NCH_3).

4.3. X-ray crystal structure determination

Crystallographic and experimental details of data collection and crystal structure determinations are given in Tables 4 and 5. Suitable crystals of **2**, **4**, **5**, **6** and **7** were selected and coated in FOMBLIN oil under an inert atmosphere. Crystals were then mounted on a loop and the data for compounds **1**, **2** and **4**–**7** were collected using graphite-monochromated Mo Kα (α = 0.71073 Å) on a Bruker AXS-KAPPA APEX II area detector diffractometer equipped with an Oxford Cryosystem open-flow nitrogen cryostat, and data were collected at 150 K. Cell parameters were retrieved using Bruker SMART software and refined using Bruker SAINT on all observed reflections. Absorption corrections were applied using SADABS [31]. The structures were solved by direct methods using either SHELXS-97 [32] or SIR 97 [33] and refined using full-matrix least squares refinement against F^2 using SHELXL-97 [32] All programs are included in the package of programs WINGX-version 1.64.05 [34].

All non-hydrogen atoms were refined anisotropically and all hydrogen atoms were placed in idealized positions and allowed to refine riding on the parent carbon atom. The molecular structures were drawn with ORTEP3 for Windows [34].

From a C_6D_6 solution of compound **1** another single crystal was obtained and subjected to X-ray diffraction analysis. The obtained structure showed a molecule of **1** co-crystallized with a C_6D_6 molecule. Crystallographic data for complexes **1**, **1**.C_6D_6, **2** and **4**–**7** were deposited in CCDC. Crystallographic data for **1**.C_6D_6 and **6b**, molecular diagram representation of **2b** and **6a**-**1** and coordination polyhedron for **6a**-**1**.

Acknowledgements

The authors are grateful to Fundação para a Ciência e a Tecnologia (FCT) for funding (PTDC/QUI/66187/2006, PTDC/QUI-QUI/109846/2009, PEst-OE/QUI/UI0100/2011, RNEM/Portuguese Mass Spectrometry Network-ITN Node (REDE/1503/REM/2005), PhD grant SFRH/BD/44295/2008 and “Ciência 2008” Programme) and to the Portuguese NMR Network (IST-UTL) for providing access to the NMR facilities.

Appendix A. Supplementary material

CCDC 865826–865833 contain the supplementary crystallographic data for this paper. These data can be obtained free of charge from The Cambridge Crystallographic Data Centre via www.ccdc.cam.ac.uk/data_request/cif.

Appendix B. Supplementary data

Supplementary data related to this article can be found at http://dx.doi.org/10.1016/j.jorganchem.2012.12.026.

References

[1] (a) O. Runte, T. Priermeier, R. Anwander, Chem. Commun. (1996) 1385–1386;
(b) W.J. Evans, C.H. Fujimoto, J.W. Ziller, Chem. Commun. (1999) 311–312;
(c) C.X. Cai, L. Toupet, C.W. Lehmann, J.F. Carpentier, J. Organomet. Chem. 683 (2003) 131–136;
(d) C.-X. Cai, A. Amgoune, C.W. Lehmann, J.F. Carpentier, Chem. Commun. (2004) 330–331;
(e) F.M. Kerton, A.C. Whitwood, C.E. Willans, Dalton Trans. (2004) 2237–2244;
(f) C.L. Boyd, T. Toupance, B.R. Tyrrel, B.D. Ward, C.R. Wilson, A.R. Cowley, P. Mountford, Organometallics 24 (2005) 309–330;
(g) F. Bonnet, A.R. Cowley, P. Mountford, Inorg. Chem. 44 (2005) 9046–9055;
(h) X. Liu, X. Shang, T. Tang, N. Hu, F. Pei, D. Cui, X. Chen, X. Jing, Organometallics 26 (2007) 2747–2757;
(i) K. Nie, X. Gu, Y. Yao, Y. Zhang, Q. Shen, Dalton Trans. (2010) 6832–6840;
(j) S. Barroso, J. Cui, J.M. Carretas, A. Cruz, I.C. Santos, M.T. Duarte, J.P. Telo, N. Marques, A.M. Martins, Organometallics 28 (2009) 3449–3458;
(k) A. Amgoune, C.M. Thomas, T. Roisnel, J.F. Carpentier, Chem. Eur. J. 12 (2006) 169–179;
(l) C.E. Williams, M.A. Sinenkov, G.K. Fukin, K. Sheridan, J.M. Lynam, A. Trifonov, F.M. Kerton, Dalton Trans. (2008) 3592–3598;
(m) M. Bouyahyi, N. Ajellal, E. Kirillov, C.M. Thomas, J.F. Carpentier, Chem. Eur. J. 17 (2011) 1872–1883.

[2] (a) Y. Yao, M. Ma, X. Xu, Y. Zhang, Q. Shen, W.-T. Wong, Organometallics 24 (2005) 4014–4020;
(b) Y. Luo, W. Li, D. Lin, Y. Yao, Y. Zhang, Q. Shen, Organometallics 29 (2010) 3507–3514;
(c) Z. Zhang, X.P. Xu, W.Y. Li, Y.M. Yao, Y. Zhang, Q. Shen, Y.J. Luo, Inorg. Chem. 48 (2009) 5715–5724;
(d) X. Xu, Z. Zhang, Y. Yao, Y. Zhang, Q. Shen, Inorg. Chem. 46 (2007) 9379–9388.

[3] (a) H. Ma, T.P. Spaniol, J. Okuda, Dalton Trans. (2003) 4770;
(b) H. Ma, T.P. Spaniol, J. Okuda, Inorg. Chem. 47 (2008) 3328–3339.

[4] (a) A. Amgoune, C.M. Thomas, S. Ilinca, T. Roisnel, J.F. Carpentier, Angew. Chem. Int. Ed. 45 (2006) 2782–2784;
(b) A. Amgoune, C.M. Thomas, J.-F. Carpentier, Macromol. Rapid Commun. 28 (2007) 693–697;
(c) M.J. Standford, A.P. Dove, Chem. Soc. Rev. 39 (2010) 486–494;
(d) C.M. Thomas, Chem. Soc. Rev. 39 (2010) 165–173;
(e) J.-F. Carpentier, Macromol. Rapid Commun. 31 (2010) 1696–1705;
(f) A. Amgoune, C.M. Thomas, J.F. Carpentier, Pure Appl. Chem. 79 (2007) 2013–2030.

[5] P.N. O'Shaughnessy, P.D. Knight, C. Morton, K.M. Gillespie, P. Scott, Chem. Commun. (2003) 1770–1771.

[6] (a) R.F. Munha, M.A. Antunes, L.G. Alves, L.F. Veiros, M.D. Fryzuk, A.M. Martins, Organometallics 29 (2010) 3753–3764;
(b) L.G. Alves, M.A. Antunes, I. Matos, R.F. Munha, M.T. Duarte, A.C. Fernandes, M.M. Marques, A.M. Martins, Inorg. Chim. Acta 363 (2010) 1823–1830;
(c) R.F. Munha, L.F. Veiros, M.T. Duarte, M.D. Fryzuk, A.M. Martins, Dalton Trans. (2009) 7494–7508;
(d) R.F. Munha, L.G. Alves, N. Maulide, M.T. Duarte, I.E. Marko, M.D. Fryzuk, A.M. Martins, Inorg. Chem. Commun. 11 (2008) 1174–1176.

[7] (a) M.A. Antunes, R.F. Munha, L.G. Alves, L.L. Schafer, A.M. Martins, J. Organomet. Chem. 696 (2011) 2–6;
(b) L.G. Alves, A.M. Martins, Inorg. Chem. 51 (2012) 10–12;
(c) R.F. Munha, J. Ballmann, L.F. Veiros, B.O. Patrick, M.D. Fryzuk, A.M. Martins, Organometallics 31 (2012) 4937–4940;
(d) L.G. Alves, F. Hild, R.F. Munhá, L.F. Veiros, S. Dagorne, A.M. Martins, Dalton Trans. (2012). http://dx.doi.org/10.1039/C2DT31133J.

[8] (a) I. Lukes, J. Kotek, P. Vojtısek, P. Hermann, Coord. Chem. Rev. 216 (2001) 287–312;
(b) N. Viola-Villegas, R.P. Doyle, Coord. Chem. Rev. 253 (2009) 1906–1925;
(c) R. Delgado, V. Felix, L.M.P. Lima, D.W. Price, Dalton Trans. (2007) 2734–2745;
(d) P. Hermann, J. Kotek, V. Kubicek, I. Lukes, Dalton Trans. (2008) 3027–3047.

[9] (a) R.E. Mewis, S.J. Archibald, Coord. Chem. Rev. 254 (2010) 1686–1712;
(b) S.P. Fricker, Chem. Soc. Rev. 35 (2006) 524–533.

[10] (a) P. Benndorf, S. Schmitt, R. Koppe, P. Ona-Burgos, A. Scheurer, K. Meyer, P.W. Roesky, Angew. Chem. Int. Ed. 51 (2012) 5006–5010;
(b) S.C. Bart, C. Anthon, F.W. Heinemann, E. Bill, N.M. Edelstein, K. Meyer, J. Am. Chem. Soc. 130 (2008) 12536–12546;
(c) O.P. Lam, P.L. Feng, F.W. Heinemann, J.M. O'Connor, K. Meyer, J. Am. Chem. Soc. 130 (2008) 2806–2816;
(d) S. Barroso, J. Cui, A.R. Dias, M.T. Duarte, H. Ferreira, R.T. Henriques, M.C. Oliveira, J.R. Ascenso, A.M. Martins, Inorg. Chem. 45 (2006) 3532–3537;
(e) H. Ferreira, A.R. Dias, M.T. Duarte, J.R. Ascenso, A.M. Martins, Inorg. Chem. 46 (2007) 750–755.

[11] (a) I. Castro-Rodriguez, K. Olsen, P. Gantzel, K. Meyer, J. Am. Chem. Soc. 125 (2003) 4565–4571;
(b) A.R. Dias, A.M. Martins, J.R. Ascenso, H. Ferreira, M.T. Duarte, R.T. Henriques, Inorg. Chem. 42 (2003) 2675–2682;
(c) A.M. Martins, J.R. Ascenso, S.M.B. Costa, A.R. Dias, H. Ferreira, J.A.B. Ferreira, Inorg. Chem. 44 (2005) 9017–9022.

[12] G. Royal, V. Dahaoui-Gindrey, S. Dahaoui, A. Tabard, R. Guilard, P. Pullumbi, C. Lecomte, Eur. J. Org. Chem. (1998) 1971–1975.

[13] (a) J. Dale, Acta Chem. Scand. 27 (1973) 1115–1158;
(b) M. Meyer, V. Dahaoui-Gindrey, C. Lecomte, R. Guilard, Coord. Chem. Rev. 178–180 (1998) 1313–1405.

[14] B. Bosnich, C.K. Poom, M.L. Tobe, Inorg. Chem. 4 (1965) 1102–1108.

[15] (a) G. Ambrosi, P. Dapporto, M. Formica, V. Fusi, L. Giorgi, A. Guerri, M. Micheloni, P. Paoli, R. Pontellini, P. Rossi, Chem. Eur. J. 9 (2003) 800–810;
(b) H. Misaki, H. Miyake, S. Shinoda, H. Tsukube, Inorg. Chem. 48 (2009) 11921–11928.

[16] X. Xu, Y. Yao, Y. Zhang, Q. Shen, Inorg. Chem. 46 (2007) 3743–3751.

[17] J. Zhang, C. Wang, M. Lu, Y.M. Yao, Y. Zhang, Q. Shen, Polyhedron 30 (2011) 1876–1883.

[18] (a) M. Ma, X. Xu, Y. Yao, Y. Zhang, Q. Shen, J. Mol. Struct. 740 (2005) 69–74;
(b) X. Xu, M. Ma, Y. Yao, Y. Zhang, Q. Shen, Eur. J. Inorg. Chem. (2005) 676–684.

[19] P.I. Binda, E.E. Delbridge, Dalton Trans. (2007) 4685–4692.

[20] T. Andrea, E. Barnea, M. Botoshansky, M. Kapon, E. Genizi, Z. Goldschmidt, M.S. Eisen, J. Organomet. Chem. 692 (2007) 1074–1080.

[21] A. Roca-Sabio, M. Mato-Iglesias, D. Esteban-Gómez, A. de Blas, T. Rodrígues-Blas, C. Platas-Iglesias, Dalton Trans. (2011) 384–392.

[22] I. Bertini, M.B.L. Janik, Y.M. Lee, C. Luchinat, A. Rosato, J. Am. Chem. Soc. 123 (2001) 4181–4188.

[23] R. Shannon, Acta Crystallogr. A32 (1976) 751–767.

[24] C.J. Schaverien, J.H.G. Frijns, J.R. van der Hende, J.H. Teuben, A.L. Spek, J. Chem. Soc. Chem. Commun. (1991) 642–644.

[25] S. Bambirra, D. van Leusen, C.G.J. tazelaar, A. Meetsma, B. Hessen, Organometallics 26 (2007) 1014–1023.

[26] B. Monteiro, D. Roitershtein, H. Ferreira, J.R. Ascenso, A.M. Martins, A. Domingos, N. Marques, Inorg. Chem. 42 (2003) 4223–4231.

[27] Y.M. Yao, Q. Shen, J. Sun, Polyhedron 17 (1998) 519–522.

[28] F.A. Kunrath, O.L. Casagrande Jr., L. Toupet, J.F. Carpentier, Polyhedron 23 (2004) 2437–2445.

[29] (a) W.A. Hermann, in: F.T. Edelman (Ed.), Synthetic Methods of Organometallic and Inorganic Chemistry, Lanthanides and Actinides, vol. 6, Verlag, Stuttgart, 1997, p. 34;
(b) G. Meyer, Inorg. Synth. 25 (1989) 146.

[30] (a) E.K. Barfield, Inorg. Chem. 11 (1972) 2273–2274;
(b) E.K. Barfield, F. Wagner, K.D. Hodges, Inorg. Chem. 15 (1976) 1370–1377.

[31] SADABS, Area-detector Absorption Correction, Siemens Industrial Automation, Inc., Madison, WI, 1996.

[32] G.M. Sheldrick, SHELXL-97: a Program for Refining Crystal Structures, Univ. of Gottingen, Germany, 1998.

[33] A. Altomare, M.C. Burla, M. Camalli, G. Cascaro, C. Giacovazzo, A. Guagliardi, A.G.G. Moliterni, G. Polidori, R. Sparna, J. Appl. Crystallogr. 32 (1999) 115.

[34] L.J. Farrugia, J. Appl. Crystallogr. 30 (1997) 565.